31

A vision-based steering control system for aerial vehicles [1]

Stéphane Viollet, Lubin Kerhuel and Nicolas Franceschini
Biorobotics Dpt., Institute of Movement Sciences, CNRS and University of the Mediterranean
France

1. Introduction

Ever since animals endowed with visual systems made their first appearance during the Cambrian era, selection pressure led many of these creatures to stabilize their gaze. Navigating in 3-D environments (Collett & Land 1975), hovering (Kern & Varju 1998), tracking mates (N. Boeddeker, Kern & Egelhaaf 2003) and intercepting prey (Olberg et coll. 2007) are some of the many behavioural feats achieved by flying insects under visual guidance. Recent studies on free-flying flies have shown that these animals are able to keep their gaze fixed in space for at least 200ms at a time, thanks to the extremely fast oculomotor reflexes they have acquired (Schilstra & Hateren 1998). In vertebrates too, eye movements are also the fastest and most accurate of all the movements.
Gaze stabilization is a difficult task to perform for all animals because the eye actuators must be both :

- fast, to compensate for any sudden, untoward disturbances.
- and accurate, because stable visual fixation is required.

In the free-flying fly, an active gaze stabilization mechanism prevents the incoming visual information from being affected by disturbances such as vibrations or body jerks (Hengstenberg 1988) (Sandeman 1980)(Schilstra & Hateren 1998). This fine mechanism is way beyond what can be achieved in the field of present-day robotics.
The authors of several studies have addressed the problem of incorporating an active gaze stabilization system into mobile robots. A gaze control system in which retinal position measurements are combined with inertial measurements has been developed (Yamaguchi & Yamasaki 1994), and its performances were assessed qualitatively while slow perturbations were being applied by hand. Shibata and Schaal (Shibata et coll. 2001) designed a gaze control system based on an inverse model of the mammalian oculomotor plant. This system equipped with a learning network was able to decrease the retinal slip 4-fold when sinusoidal perturbations were applied at moderate frequencies (of up to 0.8Hz). Another adaptive image stabilizer designed to improve the performances of robotic agents was built and its ability to cope with moderate-frequency perturbations (of up to 0.6Hz) was tested (Panerai, Metta & Sandini 2002). Three other gaze stabilization systems inspired by the

[1] Part of this paper reprinted from L. Kerhuel, S. Viollet and N. Franceschini, IROS Conference, © 2007 with permission from IEEE.

human vestibulo-ocular reflex (VOR) have also been presented (two systems for mobile robots (Lewis 1997)(Viola 1989) and one for an artificial rat (Meyer et coll. 2005)), but the performances of these systems have not yet been assessed quantitatively on a test-bed. Miyauchi et al have shown the benefits of mounting a compact mechanical image stabilizer onboard a mobile robot moving over rough terrain (Miyauchi, Shiroma & Matsuno 2008). Twombly et al. has carried out simulations on a neuro-vestibular control system designed to endow a walking robot with active image stabilization abilities (Twombly, Boyle & Colombano 2006). In the humanoid research field, some robotic developments have addressed the need to stabilize the gaze by providing robots with visuo-inertial oculomotor reflexes (e.g.: (Panerai, Metta & Sandini 2000)). Wagner et al. built a fast responding oculomotor system (Wagner, Hunter & Galiana 1992), using air bearings and bulky galvanometers. An adaptive gaze stabilization controller was recently described, but the performances of this device were measured only in the 0.5-2Hz frequency range (Lenz et al. 2008). Recently, Maini et al. succeeded in implementing fast gaze shifts on an anthropomorphic head but without using any inertial-based oculomotor reflexes (Maini et al. 2008). None of the technological solutions ever proposed so far are compatible, however, with the stringent constraints actually imposed on miniature aerial robots.

The gaze stabilization mechanisms of flying insects such as flies, are based on fine oculomotor reflexes that provide the key to heading stabilization. These high performance reflexes are of particular relevance to designing tomorrow's fast autonomous terrestrial, aerial, underwater and space vehicles. As we will see, visually mediated heading stabilization systems require:

- mechanical decoupling between the eye and the body (either via a neck, as in flies, or via the orbit, as in vertebrates' "camera eye")
- active coupling between the robot's heading and its gaze, via oculomotor reflexes
- a fast and accurate actuator. Flies control their gaze using no less than 23 pairs of micro-muscles (Strausfeld 1976)
- a visual fixation reflex (VFR) that holds the gaze steadily on the target.
- a vestibulo-ocular reflex (VOR), i.e., an active inertial reflex that rotates the eye in counter phase with the head. Flies typically use an inertial reflex of this kind which is based on the halteres gyroscopic organ, especially when performing roll movements (Hengstenberg 1988). A similar system was also developed in mammals – including humans - some hundred million years later. Rhesus monkeys' VORs are triggered in the 0.5-5Hz (Keller 1978) and even 5-25Hz (Huterer & Cullen 2002) frequency range, and are therefore capable of higher performances than humans.
- a proprioceptive sensor which is able to measure the angular position of the eye in the head or in the body. Although the question as to whether this sensor exists in the primate oculomotor system is still giving rise to some controversy (Clifford, Know & Dutton 2000)(Dancause et al. 2007), it certainly exists in flies in the form of a pair of mechanosensitive hair fields located in the neck region (Preuss & Hengstenberg 1992), which serve to measure and compensate for any head-body angular deviations in terms of pitch (Schilstra & Hateren 1998), roll (Hengstenberg 1988) and yaw (Liske 1977).

In section 2, we will describe our latest aerial robot, which has been called OSCAR II. OSCAR II differs from the original (OSCAR I) robot (Viollet & Franceschini 2001) in that its eye is no longer *mechanically coupled* to the body: this configuration makes it possible for the gaze to be actively locked onto the target, whatever disturbances may be applied to the

robot's body. In Section 3, we will describe the scheme underlying the fast, accurate control of the "eye-in-head" angle. In section 4, we will explain how we merged a gaze control system (GCS) with a heading control system (HCS). In sections 5 and 6, we will present the robot's yaw control strategy and describe the outstanding performances attained by the overall gaze and heading control systems, which are both able to counteract nasty thumps delivered to the robot's body. Finally, in section 7, we will discuss about a novel biomimetic control strategy which combines both gaze orientation and locomotion.

2. Eye-in-head or head-in-body movements : a key to forward visuomotor control

Many studies have been published on how the gaze is held still in vertebrates and invertebrates, despite the disturbances to which the head (or body) is subjected. For example, in humans, the Rotational Vestibulo Ocular Reflex (RVOR, (Miles 1998)) triggers a compensatory eye rotation of equal and opposite magnitude to the head rotation, so that the line of sight (the gaze) is stabilized. Studies on the human RVOR have shown that this inertial system responds efficiently with a latency of only about 10ms to sinusoidal head rotations with frequencies of up to 4 Hz (Tabak & Collewijn 1994) or even 6Hz (Gauthier et al. 1984), as well as to step rotations (Maas et al. 1989). Rhesus monkeys show very high VOR performances in the 0.5-5Hz (Keller 1978b) and even 5-25Hz (Huterer & Cullen 2002) frequency ranges, which means that monkeys are able to reject both slow and fast disturbances throughout this wide range of frequencies. The fly itself possesses an exquisite VOR-like reflex controlling the orientation of its head (Hengstenberg 1988). Figure 1 illustrates the outstanding performances achieved by the gaze stabilization systems of two different birds and a sandwasp. In the latter case, the authors nicely showed how the roll compensation reflex functioned in a wasp in free flight by maintaining the head fixed in space in spite of dramatic body rolls (amplitude up to 120° peak to peak) made to counter any lateral displacements (Zeil, Norbert Boeddeker & Hemmi 2008). Cancelling head roll prevents the wasp's visual system from being stimulated and therefore disturbed by rotational movements.

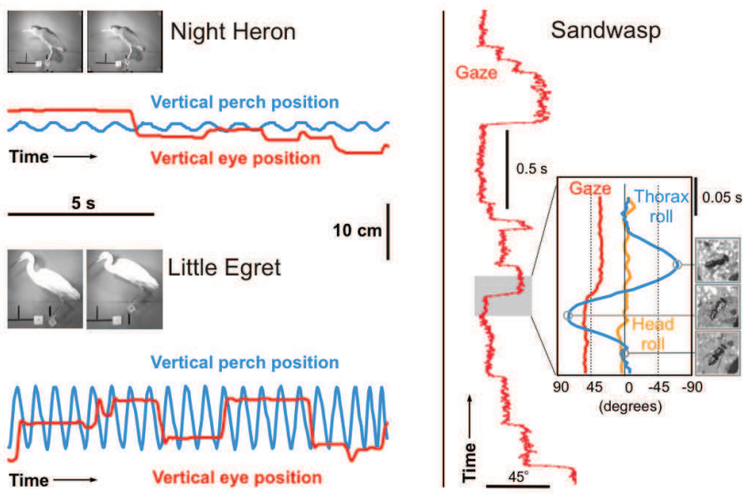

Figure 1. Gaze stabilization in birds and insects

Left: A night heron, Nycticorax nycticorax (top) and a little egret, Egretta garzetta (bottom) standing on a vertically oscillating perch. Note the long periods of perfectly stable eye position, interrupted by brief re-positioning head movements (From (Katzir et al. 2001)). Right: Horizontal gaze direction and head roll stabilization in a sandwasp (Bembix sp). Inset on the right shows thorax and head roll movements during a fast sideways translation to the left (see pictures) and a concurrent saccadic gaze shift to the right (From (Zeil, Boeddeker & Hemmi 2008)). Figure and legend reproduced from Zeil et al. with permission from Elsevier

In short, gaze stabilization seems to be a crucial ability for every animal capable of visually guided behavior. Even primitive animals such as the box jellyfish seem to be endowed with an exquisite mechanical stabilization system that holds the eyes oriented along the field of gravity (Garm et al. 2007).

3. Description of the OSCAR II robot

OSCAR II is a miniature (100-gram) cordless twin-engine aerial robot equipped with a single-axis (yaw) oculomotor mechanism (Fig. 2).

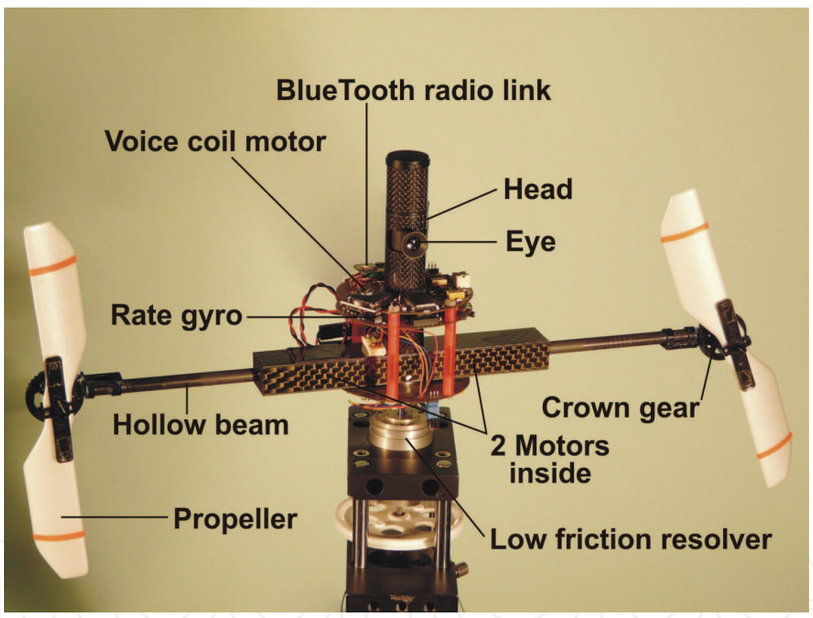

Figure 2. OSCAR II is a 100-gram aerial robot that is able to control its heading about one axis (the vertical, yaw axis) by driving its two propellers differentially on the basis of what it sees. The eye of OSCAR II is mechanically uncoupled from the head, which is itself fixed to the "body" A gaze control system (GCS in Fig. 6) enables the robot to fixate a target (a vertical white-dark edge placed 1 meter ahead) and to stabilize its gaze despite any severe disturbances (gusts of wind, slaps) that may affect its body. A heading control system (HCS in Fig. 6), combined with the GCS, makes the robot's heading catch up with the gaze, which stabilizes the heading in the gaze direction. OSCAR II is mounted on a low-friction, low-inertia resolver, so that its heading can be monitored

The robot is able to adjust its heading accurately about the yaw axis by driving its two propellers differentially via a custom-made dual sensorless speed governor (Viollet, Kerhuel

& Franceschini 2008). The robot's ”body” consists of a carbon casing supporting the two motors. This casing is prolonged on each side by a hollow carbon beam within which the propeller drive shaft can rotate on miniature ball bearings. The robot's ”head” is a large (diameter 15mm) carbon tube mounted vertically on the motor casing. Within the head, an inner carbon ”eye tube” mounted on pivot bearings can turn freely about the yaw axis.
The robot's eye consists of a miniature lens (diameter 5mm, focal length 8.5mm), behind which an elementary ”retina” composed of a single pair of matched PIN photodiodes scans the surroundings at a frequency of 10Hz by means of a fast piezo actuator (Physik Instrumente) driven by an onboard waveform generator circuit (for details, see (Viollet & Franceschini 2005)). The retinal microscanning movement adopted here was inspired by our findings on the fly’s compound eye (Franceschini & Chagneux 1997). The microscanning of the two photoreceptors occurs perpendicularly to the lens' axis, making their line-of-sights deviate periodically in concert. For details on the whys and wherefores of the particular microscanning law adopted, readers can consult our original analyses and simulations of the OSCAR sensor principle (Viollet & Franceschini 1999). Basically, we showed that by associating an exponential scan with an Elementary Motion Detector (EMD), one can obtain a genuine *Angular Position Sensor* that is able to sense the position of an edge or a bar with great accuracy within the relatively small field-of-view available (FOV = ±1.4°, which is roughly equal to that of the human fovea). Interestingly, this sensor boasts a 40-fold better angular resolution than the inter-receptor angle in the task of locating an edge, and can therefore be said to be endowed with hyperacuity (Westheimer 1981). Further details about the performances (accuracy, calibration) of this microscanning visual sensor are available in (Viollet & Franceschini 2005).

4. Implementation of the robot's oculomotor system

In the human oculomotor system, the extra-ocular muscles (EOM) are often deemed to serve contradictory functions. On the one hand, they are required to keep the gaze accurately fixated onto a steady target (Steinman 1967), and on the other hand, they are required to rotate the eye with a very small response time: a saccade of moderate amplitude is triggered within only about 100 ms (Becker 1991). Figure 3 shows a top view scheme of the novel miniature oculomotor system we have built and installed in OSCAR II (figure 2).
The high performance human oculomotor system was mimicked by controlling the orientation of the eye-tube with an unconventional extra-ocular actuator: a Voice Coil Motor (VCM), which was initially part of a hard disk microdrive (Hitachi). A VCM is normally used to displace the read-write head in disk drive control systems (Chen et al. 2006) and it works without making any trade-off between high positional accuracy and fast displacement.
As VCM control requires an efficient position feedback loop. Whereas a simple PID controller was used in the original version (Kerhuel, Viollet & Franceschini 2007), we now used a state space approach by integrating a controller composed of an estimator cascaded with a state-augmented control gain K_{e0} (cf. figure 4) computed with a classical LQG method. This structure was used to servo the angular “eye in robot” position θ_{er} to the reference input $\theta_{er\_set\text{-}point}$ (see figure 4). θ_{er} was measured by placing a tiny Hall effect sensor in front of a micro magnet ($1mm^3$) glued to the eye-tube's rotation axis.

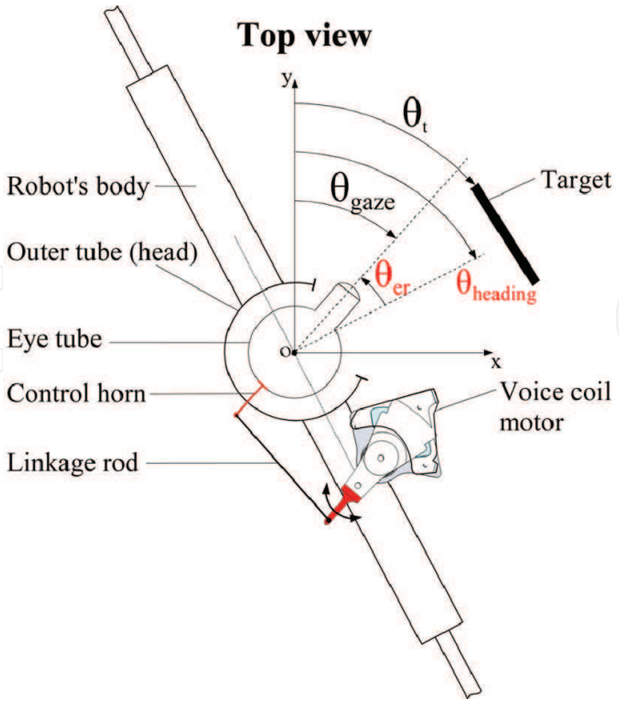

Figure 3. The OSCAR II oculomotor mechanism (top view). The central eye tube (equipped with its two-pixel piezo-scanning retina, not shown here) is inserted into a larger carbon tube (the "head"), which is mounted onto the robot's body. The eye tube is mechanically uncoupled from the head with one degree of freedom about the yaw axis. The angle θ_{er} between the robot's heading and the direction of the gaze is finely controlled (via the linkage rod and the control horn) by a micro Voice Coil Motor (VCM) that was milled out from a hard disk microdrive. The visual sensor's output is a linear, even function of $\theta_t - \theta_{gaze}$; it delivers 0 Volts when the gaze is aligned with the target (i.e., $\theta_{gaze} = \theta_t$). Adapted from (Kerhuel, Viollet & Franceschini 2007)

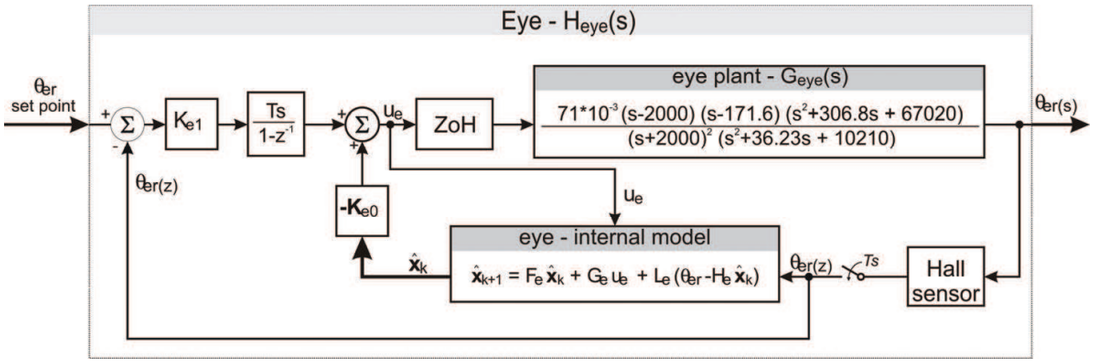

Figure 4. Block diagram of the Voice Coil Motor (VCM) servo system, which servoes the "eye in robot" angle θ_{er} (see figure 3) to the reference input $\theta_{er\_setpoint}$. In the internal state space model of the eye, both the command $U_e(z)$ and the measured angle $\theta_{er}(z)$ serve to estimate the 4 internal states of the eye's model, including its VCM actuator. The fifth external state is the integral of the eye's position error. A zero steady state error is classically obtained by augmenting the state vector and integrating the resulting angular position error

The step response shown in Figure 5 shows the very fast dynamics obtained with the closed-loop control of the eye-in-robot orientation, θ_{er}. We determined a rise time T_{rise} as small as 19ms and a settling time T_{settle} as small as 29ms (as compared to 44ms in the original version). With a 45-deg step (not shown here), a velocity peak of 2300°/s was reached, which is much higher than the 660°/s reached by our former PID controller (Kerhuel, Viollet & Franceschini 2007) and much higher than the saturation velocity (800°/s) of the human eye measured during a saccade (Maini et al. 2008). Unlike our robot's oculomotor control system (which is essentially linear), the human oculomotor control system is nonlinear, since the rise time increases typically with the saccade amplitude (Becker 1991).

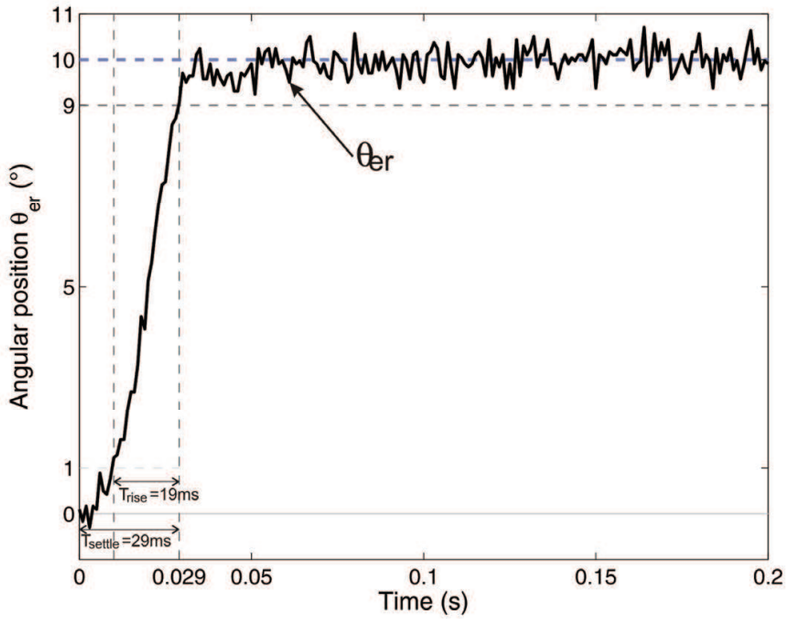

Figure 5. Closed-loop step response of the "Eye in Robot" angular position θ_{er} to a large (10 degrees) step input applied to the reference input $\theta_{er\ set\ point}$ (cf. figure 4). The voice coil motor actuator is controlled via a full state feedback controller that makes the settling time (T_{settle}) as small as 29ms. The angular position θ_{er} is measured with a miniature Hall sensor placed in front of a tiny magnet glued onto the eye's axis

5. A gaze control system that commands a heading control system

5.1 The gaze control system (GCS)

A VOR feedforward control pathway was implemented, which, like its natural counterpart, aims at counteracting any involuntary changes in heading direction. Like the semi circular canals of the inner ear, which give an estimate of the head's angular speed (Carpenter 1988), a MEMS rate gyro (analog device ADIS16100) measures the robot's body angular velocity. The VOR reflex makes θ_{er} follow any change in $\theta_{heading}$ faithfully but with opposite sign. In the frequency domain, this will occur only if the gain and phase of the transfer function relating θ_{er} to $\theta_{heading}$ are held at 0dB and 0deg, respectively, over the largest possible frequency range. This leads to the following theoretical expression for C_{VOR}:

$$C_{VOR_{th}}(s) = H_{gyro}^{-1}(s) H_{eye}^{-1}(s) \quad (1)$$

Stability problems caused by the high static gain introduced by the pseudo integrator $H^{-1}_{gyro}(s)$ led us to adopt an approximation noted $\hat{H}^{-1}_{gyro}(s)$. The expression of C_{VOR} therefore becomes:

$$C_{VOR}(s) = \hat{H}^{-1}_{gyro}(s) H^{-1}_{eye}(s) \quad (2)$$

Figure 6 shows that the control signal U_e of the eye results from the difference of two control signals:

- U_v , an angular position signal arising from the *visual* (feedback) controller.
- U_{VOR}, an angular position signal arising from the *inertial* (feedforward) controller

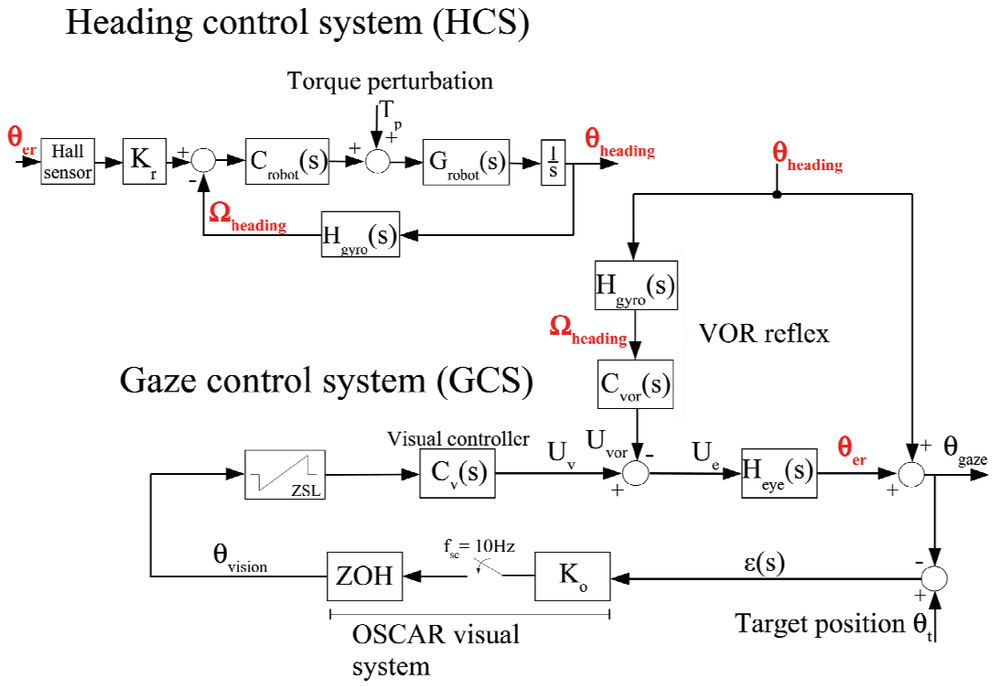

Figure 6. Block diagrams of the two interdependent control systems (an HCS and a GCS) implemented onboard the OSCAR II robot. The GCS keeps the gaze (θ_{gaze}) locked onto a stationary target (bearing θ_t), despite any heading disturbances (T_p). This system is composed of a visual feedback loop based on the OSCAR visual sensor (which acts as an "angular position sensing device") and a feedforward control system emulating the Vestibulo-Ocular-Reflex (VOR). The HCS servoes $\theta_{heading}$ to θ_{er} by adjusting the rotational speeds of the two propellers differentially. Since $\theta_{heading}$ is also an input disturbance to the GCS, any changes in heading (due to torque disturbances applied to the robot) is compensated for by a counter-rotation of the eye (θ_{er} angle). A null value of θ_{er} will mean that $\theta_{heading} = \theta_{gaze}$. Note that the two proprioceptive signals θ_{er} and $\Omega_{heading}$ given by the Hall sensor and the rate gyro (cf. Fig. 1), respectively, are used in both the GCS and the HCS. Adapted from (Kerhuel, Viollet & Franceschini 2007)

Therefore, if the robot's heading is subjected to a brisk rotational disturbance, the change in $\theta_{heading}$ will immediately be measured and compensated for by the VOR feedforward control system. The latter will impose a counter rotation of the eye of the similar amplitude but

opposite sign. In Figure 6, it can be seen that $\theta_{heading}$ also acts as an *input disturbance* to the gaze control system (GCS). The control signal U_v derived from the visual controller $C_v(s)$ adjusts the orientation θ_{er} of the eye so as to compensate for this disturbance, thus holding the gaze θ_{gaze} effectively in the direction θ_t of the visual target (that is, making $\varepsilon(s) = 0$ in Figure 6, bottom right).

We established that θ_{er} is able to follow $\theta_{heading}$ faithfully over a very large frequency range (between 1Hz and 11Hz, data not shown here). The only limitations are due to the change we made in C_{VOR} (for the sake of stability) and the approximations made during the identification of the transfer functions $H_{gyro}(s)$ and $H_{eye}(s)$.

As described in section 9 (appendix), the visual controller $C_v(s)$ (see figure 6) is an integrator. This means that the visual controller copes with any target displacement without introducing any steady state error ($\varepsilon = \theta_t - \theta_{gaze}$ in figure 6). In other words, there is no "retinal slip error" in the steady state. To prevent runaway of the eye when it loses a target, we developed a special limiter (Viollet & Franceschini 2001), which we have called a Zero-Setting Limiter (ZSL), and introduced it upstream from the visual controller (figure 6). The purpose of this nonlinear block is to clamp the error signal back to zero whenever the latter becomes higher (or lower) than a specified positive (or negative) level. At a scanning frequency of 10Hz, the OSCAR II visual sensor inevitably introduces a latency of 100ms into the visual feedback loop. This latency is the main limiting factor in the process of rejecting any fast visual disturbances to which the robot is exposed. The VOR reflex acts in a complementary manner, dramatically improving the dynamics of gaze stabilization, and thus preventing the fixated target from straying outside the (narrow) field-of-view of the eye.

5.2 The heading control system (HCS)

One of the most novel features of the present study is the fact that the visuo-inertial reflex described above was combined with the heading control system of the OSCAR II robot. The HCS was designed to take the robot's yaw dynamics, given by the transfer function $G_{robot}(s)$, into account. The HCS involves (i) a measurement of the robot's yaw angular speed $\Omega_{heading}$ (given by the rate gyro), and (ii) a proportional-integral controller (included in $C_{robot}(s)$). In the steady state, the angle θ_{er} is null, which means that the HCS makes $\theta_{heading}$ equal to θ_{gaze} (zero steady-state error). In other words, the robot's heading catches up with the gaze direction: the robot orients itself where its eye is looking.

The use of the HCS (top part of figure 6) means that the robot's orientation ($\theta_{heading}$) is servoed to the eye-in-robot orientation (θ_{er}). These two angles are therefore actively coupled. The fact that the robot "carries the eye" means that $\theta_{heading}$ constitutes both an input disturbance to the GCS based on the OSCAR visual system and an input signal to the rate gyro. It is also worth noting that the rate gyro is involved in both the VOR reflex and the speed feedback loop of the HCS (see figure 6).

To summarize, both the GCS and the HCS act in concert and share the same two proprioceptive sensors: (i) the Hall sensor that delivers θ_{er} and the rate gyro that delivers $\Omega_{heading}$. Although the GCS and HCS loops are strongly interdependent, only the HCS involves the robot's dynamics. This means that the controllers present in the GCS can be tuned by taking only the dynamics of the disturbance $\theta_{heading}$, that needs to be rejected, into account. This greatly simplifies the design of the overall control system.

6. High performance gaze stabilisation system

The overall gaze control system does not require large computational resources. The two digital controllers (one dealing with the VCM based feedback control system, and the other with the propellers speed control system (Viollet, Kerhuel & Franceschini 2008)) were built using a custom-made rapid prototyping tool designed for use with Microchip dsPIC. All the controllers involved in the VOR and the visual feedback-loop were digitized using Tustin's method and implemented in the dSPACE environment.

To test our miniature gaze and heading control system, we applied drastic torque perturbations to the robot's body. For this purpose, we built a "slapping machine" consisting of a DC motor and a light wooden arm. The arm is attached to the shaft of an electromagnetic clutch. On powering the clutch, the DC motor suddenly delivers a high acceleration thump on one side of the robot's body. The slapping machine was placed so that the arm would hit the robot and brisk thumps were thus applied to the robot repetitively was fixating a contrasting edge placed 1m from the eye.

As can be seen from the HCS block diagram (figure 6, top), any torque perturbation T_p will be compensated for by the controller C_{robot}. Meanwhile, however, the torque perturbation will have led inevitably to a change of heading. Since $\theta_{heading}$ acts as an input disturbance to the GCS (see figure 6, top of GCS), any torque perturbation is also compensated for by a counter rotation of the eye-in-robot θ_{er}. This means that the robot re-orients its heading until θ_{er} becomes null again, thus automatically bringing the heading in line with the gaze.

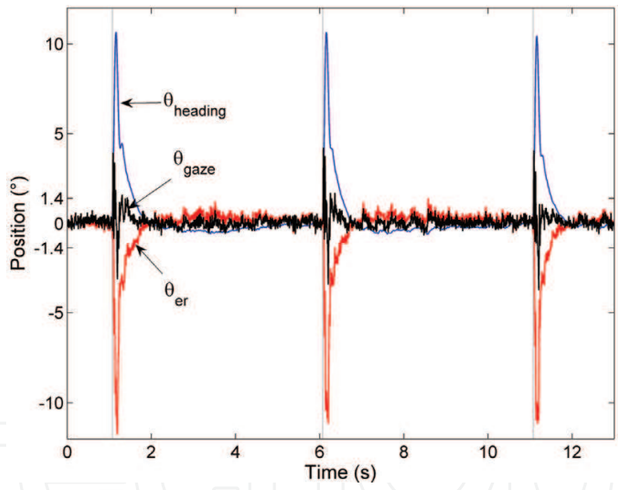

Figure 7. Reaction of the robot's orientation ($\theta_{heading}$), the "eye-in-robot" angle (θ_{er}) and the gaze (θ_{gaze}) to a sequence of 3 thumps delivered every 5 seconds (the thin vertical lines give the timing of each thump). The sudden yaw perturbation can be seen to have been counteracted swiftly, within 20ms by the VOR reflex, which succeeded in maintaining the robot's gaze (θ_{gaze}) close to the target position. The robot then reoriented itself more slowly (taking about 0.6 seconds) due to its slower body dynamics. Adapted from (Kerhuel, Viollet & Franceschini 2007)

The robot was mounted onto the shaft of a low friction, low inertia resolver which made it possible to accurately monitor the azimuthal orientation $\theta_{heading}$ (angular resolution of the resolver: 0.09°) - it should be stressed that the resolver is not involved in any control system whatsoever. As shown in Figure 7, the $\theta_{heading}$ was violently (and reproducibly) perturbed

by three sudden slaps. The eye can be seen to have swiftly counter rotated in the robot's body (curve θ_{er}), keeping the gaze (curve θ_{gaze}) virtually locked onto the target, despite this untoward perturbation.

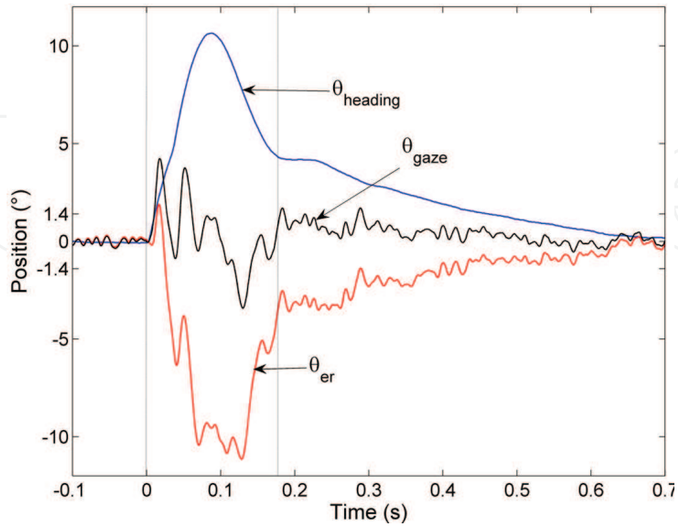

Figure 8. Magnified version of the second thump applied to the robot in figure 7. The time at which the thump was delivered is given by the left vertical line. The "eye-in-robot" profile (θ_{er} red curve) shows that the eye rotation immediately counteracts the robot's rotation ($\theta_{heading}$ blue curve), so that the gaze (θ_{gaze} black curve) remains quasi-steady. The robot's fast return phase (lasting between 0ms and 177ms) is mainly generated by the yaw rate inner loop combined with the action of the VOR. The $\theta_{heading}$ slow return phase (lasting between 177ms and 650ms) results from the control input signal θ_{er}. The VOR reflex operates quasi-instantaneously, whereas the robot's visual system has a relatively slow (10Hz) refresh rate. Adapted from (Kerhuel, Viollet & Franceschini 2007)

Figure 8 shows a close-up of the robot's eye and gaze responses to the second thump delivered as shown in figure 7. Time 0s corresponds here to the exact time when the thump was applied, as determined with a micro-accelerometer mounted at the tip of the inter-propeller beam. The robot's response can be decomposed into two phases:

- A fast phase (between 0ms and 177ms), when the perturbation was rejected, mostly by the yaw rate inner loop and the VOR via the reference input signal θ_{er} (cf. figure 6).
- A slow phase (lasting between 177ms and 650ms), when the perturbation was entirely rejected by both the VOR and the visual feedback-loop.

The eye position θ_{er} can be seen to counteract the robot's position $\theta_{heading}$ quasi perfectly (figure 8) thanks to the high speed dynamics of the eye's orientation feedback control system based on the VCM actuator. The eye's rotation is fast enough to keep the gaze θ_{gaze} locked onto the target. It is not possible to measure the robot's gaze (θ_{gaze}) directly (this would require an eye tracker or a magnetic search coil). The gaze was therefore calculated on the basis of the of the two measurable signals, $\theta_{heading}$ and θ_{er} (see figure 3):

$$\theta_{\text{gaze}} = \theta_{\text{heading}} + \theta_{\text{er}} \tag{4}$$

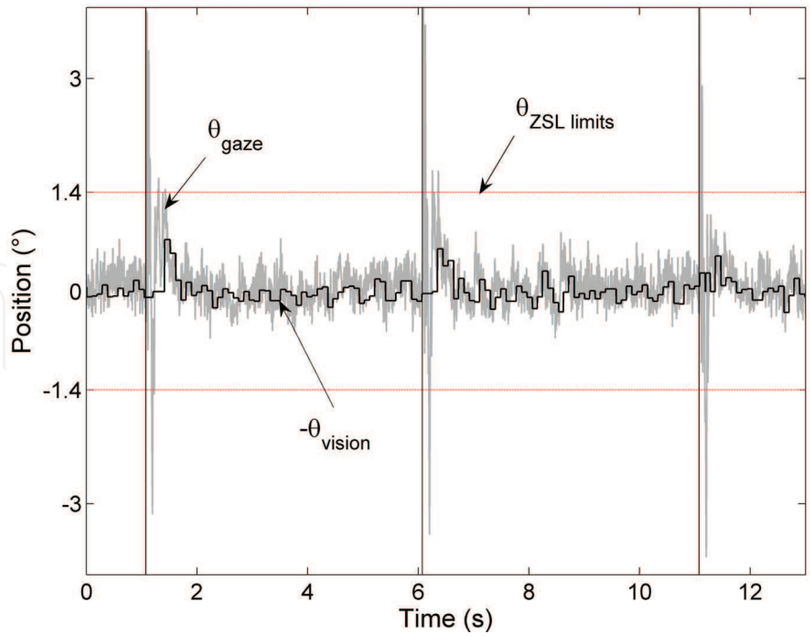

Figure 9. Gaze orientation (θ_{gaze}) compared with θ_{vision}, the gaze orientation to the target's orientation, as measured by the OSCAR sensor (see bottom left of figure 6), during the sequence of 3 thumps presented in figure 7. The two horizontal red lines delimit the field of view (±1.4°) of the eye. A gaze value greater than |1.4|° means that the target has wandered out of the field of view. The time during which the target strayed out of the visual field is so short (50ms, i.e. twice as short as the visual refresh period) that it does not impair the gaze stabilization performances. Adapted from (Kerhuel, Viollet & Franceschini 2007)

Figure 9 shows that the contrasting target (a white-dark edge) may actually wander out of the small, ±1.4° field of view of the eye for a very short time (50ms). The contrasting target keeps being "seen" by the eye-, however, as shown by the θ_{vision} signal. The reason is that the time during which the target strays out of the visual field is so short (50ms, i.e. twice as short as the visual refresh period) that it does not impair the gaze stabilization performances.

7. Steering by gazing : an efficient biomimetic control strategy.

In addition to describing the use of suitably designed oculomotor reflexes for stabilizing a robot's gaze, the aim of this study was to present a novel concept that we call "steering by gazing". Many studies have addressed the question as to how vertebrates and invertebrates use their gaze during locomotion. These studies have shown that the locomotor processes at work in many species such as humans (Wann & Swapp 2000)(Schubert et al. 2003), flying insects (Collett & Land 1975)(Schilstra & Hateren 1998)(Zeil, Norbert Boeddeker & Hemmi 2008), crabs (Paul, Barnes & Varju 1998) and even bats (Ghose & Moss 2006) involve a gaze orientation component.

Figure 10 summarizes the various feedforward and feedback control systems involved in the control of a robotic platform such as OSCAR II. The control system depicted in figure 10 is a one input (θ_{target}) and two outputs (θ_{gaze} and $\theta_{heading}$) system. The "steering by gazing" control strategy aims at making θ_{gaze} and $\theta_{heading}$ (i.e., the complete robot) to follow any variation in

θ_{target}. The mechanical decoupling between the eye and the body is here modeled by the robot block where the unique control input signal is split into one input reference for controlling the eye's orientation and one error signal for controlling the robot's heading (cf. figure 10). For a stationary target, the control system will compensate for any disturbances applied to the body by holding the gaze locked onto the target. For a moving target, the control system will change both the eye's orientation and the robot's heading to track smoothly the target.
Let us look at the path involving the "vestibulo-ocular reflex" (VOR) and the eye blocks in figure 10. On this path, the VOR feedforward control can be identified between $\theta_{heading}$ and θ_{er}. The minus sign in Σ_2 means that any rotation of the head will be compensated for by a counter rotation of the eye.
The block diagram in figure 10 also shows two feedback loops controlling both a fast plant (the eye) and a slow plant (the robot's body):

- the eye's orientation is controlled by the *visual feedback-loop* (upper closed-loop in figure 10) and the *feedfoward control* based on the VOR block.
- the robot's heading is controlled by an *inertial feedback-loop* (lower closed-loop in figure 10) based on an estimate of the heading deduced from the robot's rotational speed measured by a rate gyro.

As shown in figure 10, these two control feedback-loops are merged by using the summer Σ_2 where the estimated robot's heading ($\hat{\theta}_{heading}$) becomes an *input disturbance* for the visual feedback-loop, whereas the retinal error becomes a *reference input* ($\theta_{heading\_ref}$) for the inertial feedback-loop.

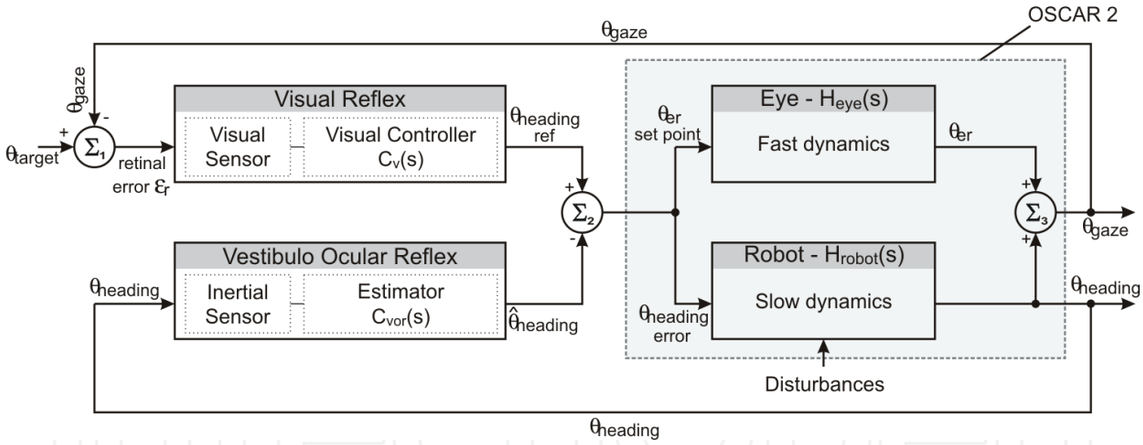

Figure 10. Generic block diagram of the "steering by gazing" control strategy. This is a control system where the input is the angular position of the target θ_{target} and its two outputs are the gaze orientation θ_{gaze} and the robot's heading $\theta_{heading}$. This system can be described in terms of Main-Vernier loops (Lurie & Enright 2000) where the reference input received by the slow heading feedback-loop is the $\theta_{heading\_ref}$ provided by the fast visual feedback loop (θ_{gaze}). This novel control system meets the following two objectives:
- keeping the gaze locked onto the visual target in spite of the aerodynamical disturbances (gusts of wind, ground effects, etc.) to which the robot is subjected
- automatically realigning the robot's heading $\theta_{heading}$ in line with the orientation of its gaze.

To summarize, the general control scheme presented in figure 10 enables any sighted vehicle:

- to hold its gaze locked onto a contrasting target such as an edge
- to stabilize its gaze despite any disturbances generated during its locomotion ("gaze stabilization")
- to track a moving target smoothly ("smooth pursuit")
- to orient or reorient its heading automatically in the line of sight, and hence toward the target ("steering by gazing")

8. Conclusion

Here we have described how a miniature tethered aerial platform equipped with a one-axis, ultrafast accurate gaze control system inspired by highly proficient, long existing natural biological systems was designed and implemented. The seemingly complex gaze control system (figure 6) was designed to hold the robot's gaze fixated onto a contrasting object in spite of any major disturbances undergone by the body. It was established that after being destabilized by a nasty thump applied to its body (cf. figures. 7,8 and 9), the robot:

- keeps fixating the target (despite the small visual field of its eye, which is no larger than that of the human fovea)
- reorients its heading actively until it is aligned with the gaze direction

Reorientation is achieved rapidly, within about 0.6 seconds (figure 8). The important point here is that the gaze itself is the fundamental (Eulerian) reference parameter, on which all the relevant motor actions (orienting the "eye in robot" and the "robot in space") are based.

This study considerably extends the scope of a former study, in which we developed a gaze control system but did not implement it onboard a robotic platform (Viollet & Franceschini 2005). Besides, the oculomotor mechanism we are now using is a novel version based on a voice coil motor (VCM) taken from a hard disk microdrive. This actuator, which is able to orient the gaze with a settling time as short as 19ms (figure 5) (i.e., faster than a human ocular saccade), was the key to the development of our ultrafast gaze stabilization system.

The two control systems (HCS and GCS) presented in figure 6 are strongly interdependent. The HCS is *actively* coupled to the GCS via the inputs θ_{er} (as measured by the Hall sensor) and $\Omega_{heading}$ (as measured by the rate gyro) it receives. Although the eye is mechanically uncoupled from the robot's body, the GCS is *passively* coupled to the HCS due to the fact that the robot carries the whole oculomotor system (and may therefore disturb the gaze orientation). By coupling the two control systems both actively and passively, we have established that the high performances of the robot's heading control system (HCS) result directly from the high performances of the gaze control system (GCS). In other words, a fast gaze stabilization is a key to fast navigation.

Our lightweight, robust gaze control system could provide a useful basis for the guidance of manned and unmanned air vehicles (UAVs) and benthic underwater (UUVs) vehicles, and especially for micro-air vehicles (MAVs) and micro-underwater vehicles (MUVs), which are particularly prone to disturbances due to fast pitch variations, wing-beats (or body undulations or fin-beats), wind gusts (or streams), ground effects, vortices, and many other kinds of unpredictable aerodynamic (or hydrodynamic) disturbances. Biological systems teach us that these disturbances can be quickly compensated for by providing robots with a visually mediated gaze stabilization system. In biological systems, locomotion is often based on visually-guided behavior where the gaze orientation plays the role of the pilot. The

generic control scheme (figure 10) presented here is in an attempt to model this biomimetic "steering by gazing" strategy.

9. Appendix

$H_{gyro}(s) = K_g \frac{(\tau_2 s + 1)}{(\tau_1 s + 1)}$	With $\tau_1 = 4.3 * 10^{-3}$s , $\tau_2 = 1897.5$s and $K_g = 2.27 * 10^{-3}$
$\hat{H}^{-1}_{gyro}(s) = K_{ginv} \frac{(\tau_5 s + 1)}{(\tau_6 s + 1)}$	With $\tau_5 = 3.68 * 10^{-3}$s , $\tau_6 = 2.31$s and $K_{ginv} = 606.5$
$H_{eye}(s) = K_e \frac{(\tau_4 s + 1)}{(\tau_3 s + 1)}$	With $\tau_3 = 18.7 * 10^{-3}$s , $\tau_4 = 0.5 * 10^{-3}$s and $Ke = 226.3$
$H_{robot}(s) = \frac{K_r}{\frac{1}{W_r^2} s^2 + \frac{2\zeta_r}{W_r} s + 1}$	With $W_r = 39.9\, rad\, s^{-1}$, $\zeta_r = 0.27$ and $K_r = 0.7889$
$K_r = 6$	Pure gain
$C_{robot}(s) = K_c \frac{\tau_c s + 1}{\tau_c s}$	With $\tau_c = 7.4$s and $K_c = 3.7 * 10^{-3}$
$C_{vor}(s) = \hat{H}^{-1}_{gyro}(s)\ H^{-1}_{eye}(s)$	
$C_v(s) = \frac{K_0}{s}$	With visual sampling rate $T_{sc} = 0.1s$ and $K_0 = 0.0574$

10. Acknowledgements

The authors acknowledge the assistance of M. Boyron for the design of the miniature electronic boards including the piezo driver, the EMD and the control systems. We thank F. Paganucci and Y. Luparini for their help with the mechanical construction of the eye, L. Goffart, F. Ruffier and J. Serres for fruitful discussions and comments on the manuscript. This work was supported by CNRS, University of the Mediterranean, the French National Agency for Research (ANR, RETINAE project) and the French Defence Agency (DGA).

11. References

Becker, W., 1991. Vision and visual dysfunction (Vol 8). In *GR.H.S. Carpenter* (Ed) Macmillan Press, Ltd, pp. 95-137.

Boeddeker, N., Kern, R. & Egelhaaf, M., 2003. Chasing a dummy target: smooth pursuit and velocity control in male blowflies. In *Proc. R. Soc. Lond.B 270*. pp. 393-399.

Carpenter, R.H.S., 1988. Movements of the eyes, 2nd edt. In *PION*, London.

Chen, B.M. et al., 2006. *Hard Disk Drive Servo Systems 2nd Edition*, Springer, Berlin.

Clifford, R.W., Know, P.C. & Dutton, G.N., 2000. Does extraocular muscle proprioception influence oculomotor control ? *Br. J. Ophtalmol*, 84, 1071-1074.

Collett, T.S. & Land, M.F., 1975. Visual control of flight behaviour in the hoverflySyritta pipiens L. *Journal of Comparative Physiology A: Neuroethology, Sensory, Neural, and Behavioral Physiology*, 99(1), 1—66.

Dancause N., M. D. Taylor, E. J. Plautz, J. D. Radel, T. Whittaker, R. J. Nudo and A. G. Feldman, 2007. A stretch reflex in extraocular muscles of species purportedly lacking muscle spindles. *Exp Brain Res*, 180(1), 15—21.

Franceschini, N. & Chagneux, R., 1997. Repetitive scanning in the fly compound eye. In *Gottingen Neurobiol. Conf.* Gottingen, p. 279.

Garm A., M. O'Connor, L. Parkefelt and D-E. Nilsson, 2007. Visually guided obstacle avoidance in the box jellyfish Tripedalia cystophora and Chiropsella bronzie. *J Exp Biol*, 210(Pt 20), 3616—3623.

Gauthier, G.B. et al., 1984. High-frequency vestibulo-ocular reflex activation through forced head rotation in man. *Aviat Space Environ Med*, 55(1), 1—7.

Ghose, K. & Moss, C.F., 2006. Steering by hearing: a bat's acoustic gaze is linked to its flight motor output by a delayed, adaptive linear law. *J Neurosci*, 26(6), 1704—1710.

Hengstenberg, R., 1988. Mechanosensory control of compensatory head roll during flight in the blowfly Calliphora erythrocephala Meig. *J. Comp Physiol A*, 163, 151-165.

Huterer, M. & Cullen, K.E., 2002a. Vestibuloocular reflex dynamics during high-frequency and high acceleration rotations of the head on body in rhesus monkey. *J Neurophysiol*, 88, 13-28.

Katzir, G. et al., 2001. Head stabilization in herons. *J Comp Physiol [A]*, 187(6), 423—432.

Keller, E.L., 1978. Gain of the vestibulo-ocular reflex in monkey at high rotational frequencies. *Vis. Res.*, 18, 311-115.

Kerhuel, L., Viollet, S. & Franceschini, N., 2007. A sighted aerial robot with fast gaze and heading stabilization. In *Intelligent Robots and Systems, 2007. IROS 2007. IEEE/RSJ International Conference on*. p. 2634—2641.

Kern, R. & Varju, D., 1998. Visual position stabilization in the hummingbird hawk moth, Macroglossum stellatarum L. *J Comp Physiol A 182*, 225-237.

Lenz, A. et al., 2008. An adaptive gaze stabilization controller inspired by the vestibulo-ocular reflex. *Bioinspir Biomim*, 3(3), 35001.

Lewis, A., 1997. Visual navigation in a robot using Zig-Zag behavior. In *Proceedings of Neural Informations Processing Systems (NIPS)*. pp. 822-828.

Liske, E., 1977. The influence of head position on the flight behaviour of the fly, Calliphora Erythrocephala. *J. Insect Physiol*, 23, 375-179.

Lurie, B. & Enright, P., 2000. *Classical feedback control with Matlab* M. Dekker, éd., Marcel Dekker.

Maas E. F., W. P. Huebner, S. H. Seidman and R. J. Leigh, 1989. Behavior of human horizontal vestibulo-ocular reflex in response to high-acceleration stimuli. *Brain Res*, 499(1), 153—156.

Maini E., Manfredi L., Laschi C., and Dario P., 2008. Bioinspired velocity control of fast gaze shifts on a robotic anthropomorphic head. *Autonomous Robots*, 25(1), 37—58.

Meyer, J.-A., Guillot A., Girard B., Khamassi M., Pirim P., and Berthoz A., 2005. The Psikharpax project: towards building an artificial rat. *Robotics and Autonomous Systems*, 50(4), 211-223.

Miles, F.A., 1998. The neural processing of 3-D visual information: evidence from eye movements. *Eur J Neurosci*, 10(3), 811—822.

Miyauchi, R., Shiroma, N. & Matsuno, F., 2008. Compact Image Stabilization System Using Camera Posture Information. *J of field robotics*, 25, 268-283.

Olberg, R.M. et al., 2007. Eye movements and target fixation during dragonfly prey-interception flights. *J Comp Physiol A Neuroethol Sens Neural Behav Physiol*, 193(7), 685—693.

Panerai, F., Metta, G. & Sandini, G., 2002. Learning visual stabilization reflexes in robots with moving eyes. *Neurocomputing*, 48, 323-337.

Panerai, F., Metta, G. & Sandini, G., 2000. Learning VOR-like stabilization reflexes in robots. In *ESANN'2000 Proceedings*. Bruges,Belgium, pp. 95-102.

Paul, Barnes & Varju, 1998. Roles of eyes, leg proprioceptors and statocysts in the compensatory eye movements of freely walking land crabs (Cardisoma guanhumi) . *J Exp Biol*, 201 (Pt 24), 3395—3409.

Preuss, T. & Hengstenberg, R., 1992. Structure and kinematics of the prosternal organs and their influence on head position in the blowfly Calliphora erythrocephala Meig. *J Comp Physiol A 171*, 483-493.

Sandeman, D., 1980. Head Movements in Flies (Calliphora) Produced by Deflexion of the Halteres. *J Exp Biol*, 85(1), 43—60.

Schilstra, C. & Hateren, J.H.V., 1998. Stabilizing gaze in flying blowflies. *Nature*, 395(6703), 654.

Schubert M., C. Bohner, W. Berger, M. Sprundel and J. E J Duysens, 2003. The role of vision in maintaining heading direction: effects of changing gaze and optic flow on human gait. *Exp Brain Res*, 150(2), 163—173.

Shibata T., Tabata H. , Schaal S. and Kawato M., 2001. Biomimetic gaze stabilization based on feedback-error-learning with nonparametric regression networks. *Neural Networks*, 14, 201-216.

Steinman, R.M., 1967. Voluntary Control of Microsaccades during Maintained Monocular Fixation. *Sciences*, 155, 1577-1579.

Strausfeld, N., 1976. *Atlas of an Insect Brain*, Springer-Verlag, Berlin, Heidelberg.

Tabak, S. & Collewijn, H., 1994. Human vestibulo-ocular responses to rapid, helmet-driven head movements. *Exp Brain Res*, 102(2), 367—378.

Twombly, X., Boyle, R. & Colombano, S., 2006. Active Stabilization of Images Acquired on a Walking. In *Advances in visual computing. Part I-II : Second international symposium, ISVC 2006*. pp. 851-860.

Viola, P., 1989. Neurally inspired plasticity in oculomotor processes. In *Proceedings of Neural Informations Processing Systems (NIPS)*. pp. 290-297.

Viollet, S. & Franceschini, N., 2005. A high speed gaze control system based on the Vestibulo-Ocular Reflex. *Robotics and Autonomous systems*, 50, 147-161.

Viollet, S. & Franceschini, N., 1999. Biologically-inspired visual scanning sensor for stabilization and tracking. In *Intelligent Robots and Systems, 1999. IROS '99. Proceedings. 1999 IEEE/RSJ International Conference on*. p. 204—209vol.1.

Viollet, S. & Franceschini, N., 2001. Super-accurate visual control of an aerial minirobot. In *Autonomous minirobots for research and edutainment, AMIRE.*

Viollet, S., Kerhuel, L. & Franceschini, N., 2008. A 1-gram dual sensorless speed governor for micro-air vehicles. In *Control and Automation, 2008 16th Mediterranean Conference on*. p. 1270—1275.

Wagner, R., Hunter, I.W. & Galiana, H.L., 1992. A Fast Robotic Eye/head System: Eye Design and Performance. In *Proc. of IEEE Engineering in Medicine and Biology Society*. pp. 1584-1585.

Wann, J.P. & Swapp, D.K., 2000. Why you should look where you are going. *Nat Neurosci*, 3(7), 647—648.

Westheimer, G., 1981. *Visual hyperacuity*, Berlin: Ottoson, Sensory Physiology 1, Springer.

Yamaguchi, T. & Yamasaki, H., 1994. Velocity Based Vestibular-Visual Integration in Active Sensing System. In *Proc. IEEE Intern. Conf. on Multisensor Fusion and Integration for Intelligent System*. Las Vegas, USA, pp. 639-646.

Zeil, J., Boeddeker, N. & Hemmi, J.M., 2008. Vision and the organization of behaviour. *Curr Biol*, 18(8), R320—R323.

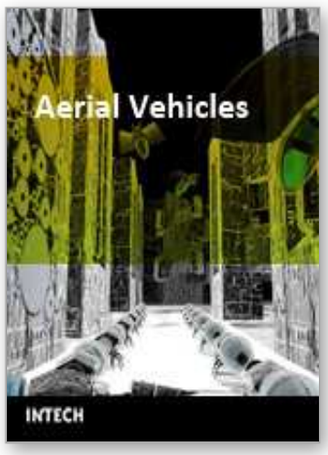

Aerial Vehicles

Edited by Thanh Mung Lam

ISBN 978-953-7619-41-1
Hard cover, 320 pages
Publisher InTech
Published online 01, January, 2009
Published in print edition January, 2009

This book contains 35 chapters written by experts in developing techniques for making aerial vehicles more intelligent, more reliable, more flexible in use, and safer in operation.It will also serve as an inspiration for further improvement of the design and application of aeral vehicles. The advanced techniques and research described here may also be applicable to other high-tech areas such as robotics, avionics, vetronics, and space.

InTech Europe
University Campus STeP Ri
Slavka Krautzeka 83/A
51000 Rijeka, Croatia
Phone: +385 (51) 770 447
Fax: +385 (51) 686 166
www.intechopen.com

InTech China
Unit 405, Office Block, Hotel Equatorial Shanghai
No.65, Yan An Road (West), Shanghai, 200040, China
中国上海市延安西路65号上海国际贵都大饭店办公楼405单元
Phone: +86-21-62489820
Fax: +86-21-62489821

IntechOpen